Biomedicine & Pharmacotherapy 167 (2023) 115474

Contents lists available at ScienceDirect

Biomedicine & Pharmacotherapy

journal homepage: www.elsevier.com/locate/biopha

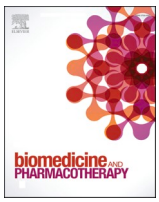

Effect of nanocapsules containing docosahexaenoic acid in mice with chronic inflammation

Matheus de Castro Leão [a], Isabella di Piazza [a], Sarah Jorge Caria [a], Milena Fronza Broering [b], Sandra Helena Poliselli Farsky [b], Mayara Klimuk Uchiyama [c], Koiti Araki [c], Kennedy Bonjour [d], Bruno Cogliati [d], Adriana Raffin Pohlmann [e], Silvia Stanisçuaski Guterres [f], Inar Alves Castro [a,*]

[a] Department of Food and Experimental Nutrition, Faculty of Pharmaceutical Sciences, University of São Paulo, São Paulo, São Paulo, Brazil
[b] Department of Clinical & Toxicological Analyses, School of Pharmaceutical Sciences, University of São Paulo, São Paulo, São Paulo, Brazil
[c] Department of Fundamental Chemistry, Institute of Chemistry, University of São Paulo, São Paulo, São Paulo, Brazil
[d] Department of Pathology, School of Veterinary Medicine and Animal Science, University of São Paulo, São Paulo, São Paulo, Brazil
[e] Department of Organic Chemistry, Institute of Chemistry, Federal University of Rio Grande do Sul, Porto Alegre, Rio Grande do Sul, Brazil
[f] Department of Production and Drugs Control, Pharmaceutical Faculty, Federal University of Rio Grande do Sul, Porto Alegre, Rio Grande do Sul, Brazil

ARTICLE INFO

Keywords:
Atherosclerosis
Nanocapsules
DHA
Inflammation
Omega 3
Cytokines

ABSTRACT

Background: Omega 3 fatty acids, such as docosahexaenoic acid (DHA) have been widely consumed as supplements to control chronic inflammation. Nanocapsules containing DHA (MLNC-DHA-a1) were developed and showed excellent stability. Thus, our objective was to evaluate the effect of MLNC-DHA-a1 nanocapsules on biomarkers of chronic inflammation.

Methods: Cells viability was determined by flow cytometry. The uptake of MLNC-DHA-a1 nanocapsules by macrophages and their polarization were determined. *In vivo*, *LDLr* $^{(-,-)}$ mice were fed a Western diet to promote chronic inflammation and were treated with MLNC-DHA-a1 nanocapsules, intravenously injected via the caudal vein once a week for 8 weeks.

Results: MLNC-DHA-a1 nanocapsules decreased the concentration of TNFα ($p = 0.02$) in RAW 264.7 cells compared to the non-treated group (NT), with no changes in IL-10 ($p = 0.29$). The nanocapsules also exhibited an increase in the M2 (F4/80^{+} CD206) phenotype ($p < 0.01$) in BMDM cells. *In vivo*, no difference in body weight was observed among the groups, suggesting that the intervention was well tolerated. However, compared to the CONT group, MLNC-DHA-a1 nanocapsules led to an increase in IL-6 (90.45 ×13.31 pg/mL), IL-1β (2.76 ×1.34 pg/mL) and IL-10 (149.88 ×2.51 pg/mL) levels in plasma.

Conclusion: MLNC-DHA-a1 nanocapsules showed the potential to promote *in vitro* macrophage polarization and were well-tolerated *in vivo*. However, they also increased systemic pro-inflammatory cytokines. Therefore, considering that this immune response presents a limitation for clinical trials, further studies are needed to identify the specific compound in MLNC-DHA-a1 that triggered the immune response. Addressing this issue is essential, as MLNC-DHA-a1 tissue target nanocapsules could contribute to reducing chronic inflammation.

1. Introduction

Chronic inflammatory conditions lead to several diseases that collectively represent the leading causes of disability and mortality worldwide, such as cardiovascular disease, cancer, diabetes mellitus, chronic kidney disease, non-alcoholic fatty liver disease, autoimmune and neurodegenerative disorders [1–4]. In these examples, the long-lasting chronic inflammation is a result of the signaling promoted by cells of the innate and adaptive immune system, as response to the presence of damage-associated molecular patterns (DAMPs) in the blood stream or inside the host cells and tissues [1,5].

The reaction of the immune system cells to various types of DAMPs is complex and difficult of controlling. For this reason, in many cases, due to discomfort, pain or even risk of more severe complications, the

* Correspondence to: LADAF, Department of Food and Experimental Nutrition, Faculty of Pharmaceutical Sciences, University of São Paulo, Av. Lineu Prestes, 580, B14, Zip Code: - 05508–900, São Paulo, São Paulo, Brazil.
E-mail address: inar@usp.br (I.A. Castro).

https://doi.org/10.1016/j.biopha.2023.115474
Received 28 June 2023; Received in revised form 6 September 2023; Accepted 7 September 2023
Available online 21 September 2023

systemic inflammation is suppressed by drugs. However, non-steroidal anti-inflammatory drugs (NSAIDs) or glucocorticoids, have many adverse effects [6–10], and their continuous intake can increase the individual susceptibility to infections [11,12].

In this context, pharmacological strategies based on bioactive compounds could provide an interesting alternative to complement drug prescriptions, thereby improving the quality of life for patients. Among the bioactive lipids, it has been reported the anti-inflammatory effects attributed to omega-3 fatty acids, particularly eicosapentaenoic acid (C20:5 n3; EPA) and docosahexaenoic acid (C22:6 n3; DHA) [13]. EPA and DHA exert anti-inflammatory activity by replacing arachidonic acid (AA) in the phospholipids, leading to produce less potent prostaglandins, prostacyclins, leukotrienes and thromboxanes after the activation of cyclooxigenases (COX) and lipoxygenases (LOX) [13,14]. In addition, EPA and DHA can inhibit the translocation of the nuclear factor NF-kappaB (NFkB) to the nucleus through Peroxisome proliferator-activated receptor gamma (PPARγ) depending mechanisms, reducing the expression of genes encoding pro-inflammatory molecules [14–16]. It has also been reported that EPA and DHA suppress the inflammasome pathway, decreasing the Interleukin 1β (IL1β) maturation and release, and they can also serve as substrates for the synthesis of specialized pro-resolving mediators (SPMs), such as resolvins, protectins and maresins, capable of resolving the inflammatory process [2,3,17–19]. In fact, EPA and DHA may posses preventive and therapeutic potential in managing chronic inflammatory diseases [16], and new-nanotechnology-based strategies have been developed to deliver omega − 3 fatty acids to target tissues [20].

On the other side, strategies involving general immunosuppression have shown some important limitations, because inflammation is essential to protect individuals also against pathogens–associated molecular patterns (PAMPs) and damage-associated molecular patterns (DAMPs) [1,2]. One example is a study published by Ridcker et al., in which patients with cardiovascular disease treated with Interleukin-1β monoclonal antibody showed a reduction of cardiovascular events, but had more infections caused by the systemic suppression of the immune system [21]. Thus, it is necessary to develop alternatives for reducing chronic inflammation without inhibiting the immune system's ability to protect the body against new infections. One alternative is the application of nanotechnology-based drug delivery systems to deliver anti-inflammatory compound straightly to the target tissue. Nanoparticle-mediated drug delivery systems have been used in anti-inflammatory therapies, reducing medical dosage and improving therapeutic effectiveness [22].

In a previous study carried out by our group [23], anti-PECAM-1-surface-functionalized metal-complex multi-wall nanocapsules containing DHA richer algae oil in their core (MLNC-DHA-a1) were developed, showed a 94.80% conjugation efficiency and did not show significant toxicity towards HUVEC cells. Thus, our hypothesis, as summarized in Fig. 1, is that MLNC-DHA-a1 nanocapsules could be engulfed by the macrophage as a DAMP, their lipid content hydrolyzed by lysosomal lipases, releasing non-esterified fatty acids (NEFA) such as DHA for generation of lipid mediators [24]. Upon Toll-like receptor 4 (TLR4) activation, there is a rapid decrease in the cellular content of polyunsaturated fatty acids due to increased phagocytic activity, endoplasmic reticulum enlargement and synthesis of oxylipins [25]. Thus, it is supposed that the DHA supplied by our nanocapsules can be rapidly oxidized by cyclooxygenase, 5-lipoxygenase and cytochrome P450 (CYP), leading to the synthesis of anti-inflammatory oxylipins, including Specialized Pro-Resolving Mediators (SPMs) [25,26]. SPMs modulate the phenotype conversion of M1 into M2 macrophages, contributing to the resolution of inflammation [27]. In addition, the increase of DHA/AA ratio can reduce the inflammation by other mechanisms [13].

Given the hypothesis outlined in Fig. 1, it is important to evaluate the cytotoxicity, determine the *in vitro* effect of these nanocapsules on macrophage uptake and polarization, and to evaluate the tolerance of the animals to the nanocapsules injections and their inflammatory

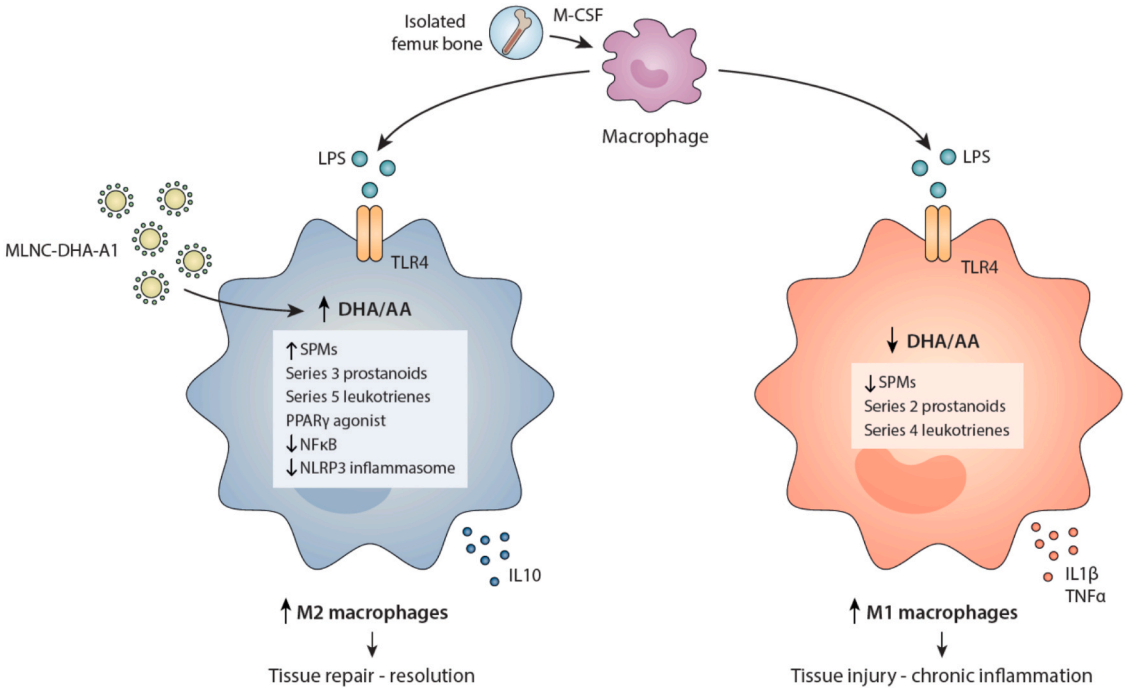

Fig. 1. Summary of the strategy proposed in this study. The surface-functionalized (anti-PECAM-1) metal-complex multi-wall nanocapsules containing algae oil as DHA source (MLNC-DHA-a1) could be internalized by the macrophages, promoting a higher DHA/AA ratio inside the cell compared with non-treated samples. As consequence, MLNC-DHA-a1 supplemented cells could show an anti-inflammatory condition associated to M2 polarization, leading to a higher plaque stability. Abbreviations: Macrophage colony-stimulating factor (M-CSF), Lipopolysaccharides (LPS), Tool Like Receptor 4 (TLR4), docosahexaenoic acid (DHA), arachidonic acid (AA), Interleukin 1β (IL 1β), Interleukin 10 (IL 10), Tumor necrosis factor-alpha (TNF-α), Peroxisome proliferator-activated receptor gamma (PPARγ), factor nuclear kappa B (NFkB), NOD-, LRR- and pyrin domain-containing protein 3 inflammasome (NLRP3) and Specialized pro-resolving mediators (SPMs).

response in plasma and liver after the treatment.

2. Material and methods

2.1. Materials

Lipid-core nanocapsules containing DHA (**LNC-DHA**), multi-wall nanocapsules containing DHA (**MLNC-DHA**) and the surface-functionalized (anti-PECAM-1) metal-complex multi-wall nanocapsules containing DHA (**MLNC-DHA-a1**) were prepared and characterized in our previous study [23] (Fig. S1**).** Algae oil applied in the oral supplementation (DHASCO™) was purchased from DSM (Heerlen, Netherlands). Medium-chain triacylglycerol (MCT) was purchased from Nutrimed Ind. Ltda (São Paulo, Brazil). Honey was supplied by Apis-Nutri Ltd. (Mandaguari, Brazil). The fatty acid composition of the algae oil and MCT were previously described in another study published by our group [23].

2.2. Methods

2.2.1. Cell culture

RAW 264.7 (immortalized murine macrophages) cells were obtained from the Rio de Janeiro Cell Bank (BCRJ, Rio de Janeiro, RJ, Brazil) and cultured in DMEM (Gibco, Grand Island, NY, USA) high glucose (4500 pg/mL) containing 10% FBS. Cells were kept at 37 ºC under a controlled CO_2 atmosphere of 5%. Cell's culture medium was replaced every 2–3 days and the cells were trypsinized with 0.01% trypsin in EDTA buffer (Vitrocell Embriolife, Campinas, SP, Brazil).

2.2.2. Cell viability

The cytotoxicity of the nanocapsules was evaluated using a flow cytometer after culturing. Briefly, cells were seeded at 2.5×10^4 cells/well in 24-well microplates (Costar® Multiple Well Cell Culture Plates, Corning, Glendale, Arizona, USA) and kept at 37 ºC for 24 h. Afterward, cells were treated with LNC-DHA; MLNC-DHA and MLNC-DHA-a1 (Fig. S1) at three concentrations: 0.14, 0.75 and 1.40×10^{11} nanoparticles/mL, and cultured for 24, 48 and 72 h. Isolated anti-PECAM-1 was also evaluated at a 200 μg/mL concentration. After that, cells were detached and washed twice in phosphate-buffered saline containing 1% bovine serum albumin. Next, cells were incubated with Annexin V (previously diluted (1:20) in Annexin V (Life Technologies, Carslabe, USA) binding buffer (10 mM N-2-hydroxyethylpiperazine-N′−2-ethanesulfonic acid, 140 mM NaCl, 25 mM $CaCl_2$, pH 7.4; BD Pharmingen, Franklin Lakes, NJ) during 20 min in the dark, at room temperature. After this, 200 μL Annexin V binding buffer and 7-AAD (1:200) were added. Data from 10,000 events were acquired in an Accuri C6 flow cytometer (BD Pharmingen), and the stained cells were analyzed. The negative double group for AnxV and 7-AAD-(non-apoptotic and non-necrotic) marking was plotted to quantify the cell viability (AnxV-, 7-ADD -), single marking with AnxV represented cells in apoptosis (AnxV+, 7-ADD -), single marking with 7-AAD indicated cells in necrosis (AnxV-, 7-ADD+), while the double group positive for AnxV-7-AAD denoted the group of cells in late apoptosis (AnxV+ , 7-ADD+). The results of triplicates were expressed as a percentage (%).

2.2.3. Real-time uptake of the nanocapsules by RAW 264.7 macrophages

The uptake of nanocapsules by macrophages was determined by enhanced dark-field hyperspectral microscopy (CytoViva®) as described by Sandri et al. [28]. First, RAW 264.7 murine macrophages (8×10^4 cells) were seeded in extra clean dust-free Nexterion® Glass D coverslips (#D263T; Schott, New York, NY, USA) present in 96-well plates (Corning, NY, USA). After adherence, cells were incubated with a medium containing MLNC-DHA and MLNC-DHA-a1 at 0.75×10^{11} nanoparticles/mL for 4 h at 37 ºC under a 5% CO_2 atmosphere. A non-treated group (NT) was kept in DMEM 10% SFB. Immediately after incubation, cells were washed three times with 5% FBS-PBS, and the coverslip was placed on extra clean dust-free Nexterion® Glass B slides (NexterionR Glass B; Schott, NY, EUA) containing 10 μL of 5% FBS-PBS. Then, 10 μL of cell solution were set up using extra clean dust-free slides (NexterionR Glass B; Schott, NY, USA) and coverslips (Nexterion Glass D #D263T; Schott). RAW 264.7 murine macrophages were imaged using a CytoViva Ultra Resolution Imaging System (CytoViva, Inc., AL, USA) mounted on an Olympus BX51 microscope (x1500 magnification; Olympus Corporation, Tokyo, Japan) equipped with fluorite 100 × oil iris 0.6–1.30 numerical aperture (NA) objective and a 75 W Xe light source. Optical images were taken using a Dage XL CCD digital camera with Image Processing Software (Dage ®; DAGE-MTI of MC, Inc., MI, USA). ImageJ software, version 2.1.0/ 1.53c (2010–2022), was used to place the scale bars. One hundred cells from representative photomicrographs were randomly chosen for this measurement and each treatment.

2.2.4. Macrophage polarization

The experiment was performed according to the method previously established by Ying et al. [29]. Initially, C57Bl/6 mice were anesthetized and euthanized to collect the left and right femurs for medullary washes collection, using an icy PBS solution containing 2% Fetal Bovine Serum (FBS). All animal experiments were conducted under the National Institutes of Health guidelines and were approved by the Institutional Animal Care and Use Committee of FCF/USP. Then the bone marrow pool was resuspended using 21 G needles to dissociate the cells and pass them through a 70 μm cell strainer to remove other tissues. The cells were washed with NH_4Cl 0.8% solution and incubated in ice for red cell removal. After centrifugation for 5 min, 500 x g at 4 °C, the cells were resuspended with bone marrow-derived macrophages (BMDM) medium, composed of IMDM (Iscove Modified Dulbecco Media), 20% L929 cell culture rich in monocyte growth factor (M-CSF) and 10% of FBS. The cells were counted and plated at the concentration of 5×10^5 cells/well in a 24-well plate and maintained in BMDM medium for 7 days for cell differentiation. After this period, and considering that this time provides 90% of macrophage differentiation, naive cells were exposed to *Escherichia coli* (LPS) 100 ng/mL and maintained for 24 h to generate the M1- inflammatory phenotype macrophage. Treatments were performed with dexamethasone (500 ng/mL), MLNC-DHA (0.75×10^{11} particles/mL) or MLNC-DHA-a1 (0.75×10^{11} particles/mL containing 200 μg/mL of Anti-PECAM-1). After 48 h, the supernatant was removed and cytokines were analyzed by ELISA assay according to the manufacturer's instructions. Single-cell suspensions were prepared at 2×10^7 cells/mL in staining buffer (10% FCS in PBS) and pre-incubated with 1 μg of the 2.4G2 antibodies for 5–10 min on ice prior to staining. About 50 μL of cell suspension (equal to 10^6 cells) were dispensed into each tube or well along with a previously determined optimal concentration of cell surface specific antibody against $F4/80^+$ CD80 and $F4/80^+$ CD206 for differentiation of M1 and M2 macrophages respectively, in 50 μL of staining buffer. Cell surface expression of these maturation markers was measured on BD opteia™ kits (BD Biosciences). The collected events were analyzed with FlowJo v7.6 (Treestar).

2.2.5. Animal protocol

Three-month-old male homozygous $LDLr^{(-/-)}$ mice in the C57BL/6 background were purchased from the Faculty of Pharmaceutical Sciences, University of São Paulo. The animals were divided into 5 groups and kept for 24 weeks under a Western diet *ad libitum*. After this period, one group (BASELINE) was euthanized (n = 10), and the diet of the other groups was replaced by AIN93M regular diet [30] for 8 weeks (Fig. S2). The animals were kept at 25 ± 2 °C and relative humidity of 55 ± 15% in an inverted cycle of 12 h light/12 h dark. Diet formulation and chemical composition is shown in Supplementary material (Table S1 and Table S2), respectively. Food intake and animal weight were weekly measured. During the last 8 weeks, **DHA-D** group (n = 9) was supplemented with algae oil by gavage. Algae oil (0.011 mL) was mixed with 0.094 mL of honey and 0.094 mL of soybean oil to reduce the gavage stress [31]. This mixture (0.20 mL) was given to each animal

once a week, and the dose was based on 1.8 g/day for humans [32]. **CONT** group (n = 11) had no supplementation. The **MLNC-DHA-a1** group (n = 15) received 5.36×10^8 surface-functionalized (anti--PECAM-1) metal-complex multi-wall nanocapsules containing 12 μL algae oil/mL and **LNC-MCT** group (n = 15) received 1.09×10^8 lipid-core nanocapsules containing 12 μL MCT/mL, intravenously injected via caudal vein once a week. The body weight of the animals at the beginning of the intervention was 47.03 ± 0.62 g. Thus, the dose of DHA provided by diet or nanocapsules were 28.57 mg ≈ 10 mg DHA Kg bw/day and 0.0011 mg ≈ 0.0004 mg DHA Kg bw/day, respectively. After this second period, mice were anesthetized with isoflurane and euthanized. Blood samples were collected after the euthanasia, transferred to EDTA (1%) vacutainer tubes, and centrifuged at 3000 x g for 10 min at 4 °C. Tissues and plasma were frozen in liquid nitrogen and stored at − 80 °C for analysis.

2.2.6. Plasma metabolites

The concentration of plasma lipids, including total cholesterol (TC), triglycerides (TG), high-density lipoprotein (HDL), low-density lipoprotein (LDL), besides glucose, aspartate transaminase (AST) and alanine transaminase (ALT) was quantified using commercial kits from Labtest Diagnóstica SA (Lagoa Santa, Brazil).

2.2.7. Inflammatory and oxidative stress biomarkers

The cytokines concentration, including interleukin-6 (IL-6), tumor necrosis factor-alpha (TNF-α), interleukin-10 (IL-10) and interleukin 1β (IL-1β), was quantified in plasma and liver homogenate, using MILLIPLEX MAP Mouse Cytokine/Chemokine Magnetic Bead Panel (MCYTOMAG-70 K) (Millipore, St. Charles, MO, USA). The protein content of the homogenates was quantified by Bradford methodology. Malondialdehyde (MDA) concentration was determined by reverse phase HPLC according to Hong et al. [33] and analyzed using a Phenomenex reverse-phase C18 analytical column (250 mm × 4.6 mm; 5 mm; Phenomenex) with an LC8-D8 pre-column (Phenomenex AJ0- 1287) coupled to an HPLC (Agilent Technologies 1200 Series). A standard curve was prepared using 1,1,3,3-Tetraethoxypropane (TEP, T9889 Sigma-Aldrich), and data were expressed as nmol/mg protein.

2.2.8. Fatty acids proportion

Fatty acids were determined in the liver homogenates and plasma according to Shirai et al. [34] using a gas chromatography coupled with a triple quadrupole mass spectrometer (GC-MS Agilent 7890 A GC System, Agilent Technologies Inc., Santa Clara, USA). Fatty acids were separated on a fused silica capillary column (J&W DB-23 Agilent Inc. Santa Clara, USA). Compounds were identified by comparing the retention time of fatty acids in the samples with the retention time of standards (FAME 37 Component Mix Supelco 47885) and also based on a comparison of their mass spectra with those given in the spectral database of the National Institute of Standards and Technology (NIST, Gaithersburg, MD, USA). One analysis was carried out/animal, and the fatty acid/IS (C23:0, Fluka 91478) area ratio was applied to calculate the percentage of each fatty acid.

2.2.9. Statistical analysis

Data were presented as mean ± SEM. Treatments were compared using one-way ANOVA and Tukey HSD post-test or non-parametric Kruskal-Wallis ANOVA by Ranks, followed by Multiple Comparisons (2-tailed). T-test or Mann-Whitney test were applied to compare BASELINE and CONT groups. A p-value of 0.05 was adopted to reject the null hypothesis. Calculations will be performed using Statistica v.13 (TIBCO Software Round Road, TX, USA). Graphs were elaborated using R Studio and GraphPad Prisma v9 (GraphPad Software, CA, USA).

3. Results

3.1. In vitro assays

The toxicity of the nanocapsules was determined using RAW 264.7 murine macrophages (Fig. 2). The results showed that the viability of the cells incubated with three concentrations of nanocapsules for 24 h (Fig. 2A), ranged from 52.36 ± 17.62% to 83.33 ± 1.59%, but did not differ among themselves ($p = 0.39$) (Fig. 2B). A similar trend was observed after 48 h (Fig. S3) and 72 h (Fig. S4). Although no statistically differences were observed, we opted to proceed with the concentration of 0.75×10^{11} nanocapsules/mL was for the subsequent assays to minimize any potential toxicological risk. Fig. 3 shows that all nanocapsules were internalized as a damage-associated molecular pattern (DAMP) by RAW 264.7 macrophages, according to the strategy proposed in our hypothesis (Fig. 1). In the next step, BMDM cells were applied to evaluate macrophage polarization. As shown in Fig. 4, internalization of MLNC-DHA and MLNC-DHA-a1, led to a reduction in TNF-α compared with NT cells ($p = 0.01$) (Fig. 4A), while no difference was observed to IL-10 ($p = 0.29$) (Fig. 4B). Regarding to macrophage polarization, treatments with dexamethasone or nanocapsules did not change the M1 phenotype ($p = 0.25$) (Fig. 4C). However, MLNC-DHA-a1 enhanced ($p < 0.01$) M2 phenotype compared with NT cells, while MLNC-DHA showed a trend to increase it ($p = 0.06$) (Fig. 4D), suggesting the beneficial effect of the nanocapsule in promoting macrophage switch phenotype.

3.2. In vivo assays

This is the first *in vivo* study that applies a surface-functionalized nanocapsule containing algae oil in the core. For this reason, our first challenge was to evaluate if weekly caudal injections could influence diet intake and, consequently, body weight gain of the animals. In our experimental protocol, all groups received a Western diet for 24 weeks. After, about two to three animals were selected from each group to compose the BASELINE (n = 10) group, while the remaining animals were divided into four groups (n = 9–15) and received a regular diet for 8 weeks. There was no difference among the groups at the beginning (25.74 ± 0.31 g, $p = 0.32$, $n = 57$), nor after 24 weeks under a Western diet containing about 36% lipids (47.03 ± 0.62 g, $p = 0.57$, $n = 56$). The same was observed among the 4 groups receiving a regular diet after 32 weeks (35.39 ± 0.65 g, $p = 0.49$, $n = 47$) (Fig. S5A). Neither Western diet (2.40 ± 0.04 g pc, $p = 0.96$) nor regular diet intake (3.02 ± 0.22 g pc, $p = 0.26$) changed according to the groups (Fig. S5B). The use of a Western diet in LDL$^{(-,-)}$ mice is a classical model for inducing inflammation and promoting lipid profile alteration. In our model, the Western diet caused the increase of TC, LDL, HDL, TG, ALT, IL-1β concentration in plasma, and TNFα ($p = 0.05$) in liver homogenate (Table S3). However, 8 weeks after discontinuing the stimulus, except for IL-1β, the other measured cytokines in plasma and liver did not change, suggesting a maladapted post-resolution condition.

After 24 weeks, the inflammatory stimulus was removed by replacing the Western diet with a regular diet, and the effect of the oral interventions with algae oil (DHA-D) and the functionalized nanocapsules (MLNC-DHA-a1) was compared in terms of lipid profile and oxidative stress. Table 1 describes the major fatty acids profiles determined in the animals after 32 weeks, both in liver homogenate and plasma. No important changes were observed in the proportion of fatty acids analyzed in plasma among the groups. In the liver, DHA-D group that received algae oil supplementation by gavage showed a higher proportion of DHA compared with CONT ($p = 0.02$), but not compared with MLNC-DHA-a1 ($p = 0.18$) (Table 1). This result suggests that some of the DHA from the surface-functionalized nanocapsules reached the liver, but it was not enough to increase DHA proportion compared to CONT ($p = 0.35$). Furthermore, no alteration was observed in the relative liver weight (0.04 ± 0.00%, $p = 0.45$).

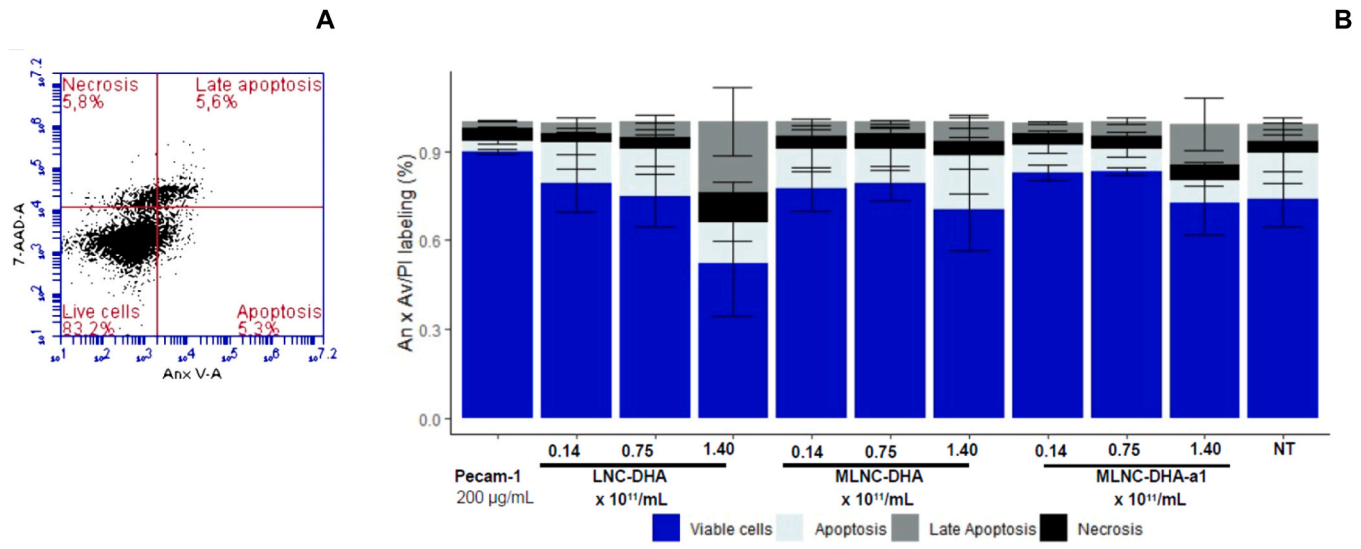

Fig. 2. RAW 264.7 murine macrophages viability, necrosis, apoptosis and late apoptosis as estimated by flow cytometry after culturing incubated with LNC-DHA, MLNC-DHA and MLNC-DHA-a1 at three concentrations (0.14 $\times 10^{11}$, 0.75 $\times 10^{11}$ and 1.40 $\times 10^{11}$ /mL), also incubated without any nanocapsules (NT) and isolated anti-PECAM-1 at 200 µg/mL for 24 h. Fig. 2A: Flow cytometry colocalization of annexin-V binding and propidium iodine uptake for quantitation of RAW 264.7 murine macrophages incubated with MLNC-DHA-a1, as example. The horizontal axis depicts fluorescein-labeled annexin V; the vertical axis shows binding of propidium iodide fluorescence. Fig. 2B: Proportion of RAW 264.7 murine macrophages viability, necrosis, apoptosis and late apoptosis. Vertical bars are mean ± SEM (n = 3). No difference was observed among the samples according to cell viability ($p = 0.34$), necrosis ($p = 0.66$), apoptosis ($p = 0.75$) and late apoptosis ($p = 0.48$) by Kruskal Wallis analysis.

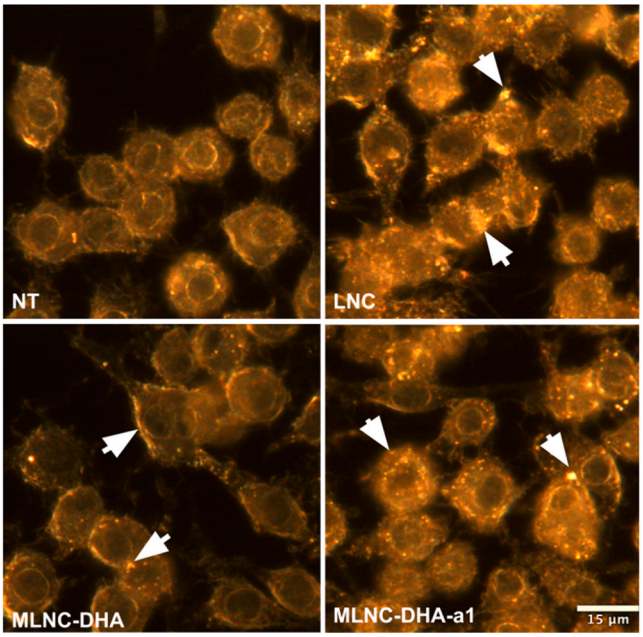

Fig. 3. Three-dimensional Cytoviva microscopy images of uptake performed in RAW 264.7 murine macrophages after 2 h of incubation with LNC-DHA, MLNC-DHA and MLNC-DHA-a1 at 0.75 $\times$ 10^{11} /mL, and also incubated without any nanocapsules (**NT**). Scale bar: 15 µm.

Given the higher proportion of polyunsaturated fatty acids in oral DHA supplementation, it was expected to potentially increase oxidative stress. However, in our model, no difference was observed in MDA concentration ($p = 0.47$) in the liver homogenate (Fig. S6). The other biomarkers measured in the groups at the end of 32 weeks did not show a significant difference (Table 2). In the subsequent analysis, a LNC-MCT group was included as a control of the MLNC-DHA-a1 group. The LNC-MCT group contained MCT instead of DHA in the lipid core. The effect of the intervention with the nanocapsules and oral supplementation on systemic cytokines is shown in Fig. 5. The MLNC-DHA-a1 group increased levels of IL-6 (Fig. 5A; $p < 0.01$), IL-1β (Fig. 5B; $p = 0.01$) but also increased IL-10 (Fig. 5C; $p < 0.01$) without altering TNFα (Fig. 5D; $p = 0.11$). No changes were observed in the cytokines determined in the liver (Table 2).

3.2.1. *Discussion*

Our data showed that lipid-core nanocapsules containing DHA (LNC-DHA), multi-wall nanocapsules containing DHA (MLNC-DHA) and the surface-functionalized (anti-PECAM-1) metal-complex multi-wall nanocapsules containing DHA (MLNC-DHA-a1) did not present toxicity when evaluated at 0.14 and 0.75 and 1.40$\times 10^{11}$ nanocapsules/mL in RAW 264.7 cells, after 24, 48 and 72 h. The toxicity and ability to be phagocyted by immune system cells is a complex subject that depends on many factors, including carrier components, excipients, impurities, therapeutic content, shape, size, elasticity, surface chemistry, and charge [35]. The nanocapsules were composed of polycaprolactone, sorbitan monostearate, zinc acetate, low molecular weight chitosan and polysorbate 80, as previously described (Fig. S1) [23]. These materials have been widely applied to synthesize nanoparticles without reported toxicity, even using animal models [36–38]. Our results confirm that the material applied to build the capsule wall and the anti-PECAM-1 applied on the surface did not affect the cells viability at 0.75$\times 10^{11}$ nanocapsules/mL. Moreover, the algae oil (DHASCO®, DSM) containing 35.13 ± 0.35 g/100 g of DHA, used to compose the lipid core, was not sterilized or depyrogenated due to its low oxidative stability. Thus, our results showed that although non-sterilized, the algae oil applied in our study can be considered relatively safe to prepare nanocapsules for further *in vivo* animal assays. However, extrapolating from *in vitro* data to *in vivo* behavior should be done cautiously [35].

Concerning phagocytosis and polarization, the shape and size of our nanocapsules may also have contributed to their internalization by RAW 264.7 macrophages. Our nanocapsules showed a spherical shape, with sizes ranging from 159.12 ± 1.25–163.50 ± 5.33 nm, and all absolute zeta potential values were below 14 mV, regardless of the negative or positive coating [23]. It has been reported that non-spherical and non-electrical charged carriers may circulate longer than similarly sized spheres, cationic or anionic nanoparticles, due to reduced recognition by

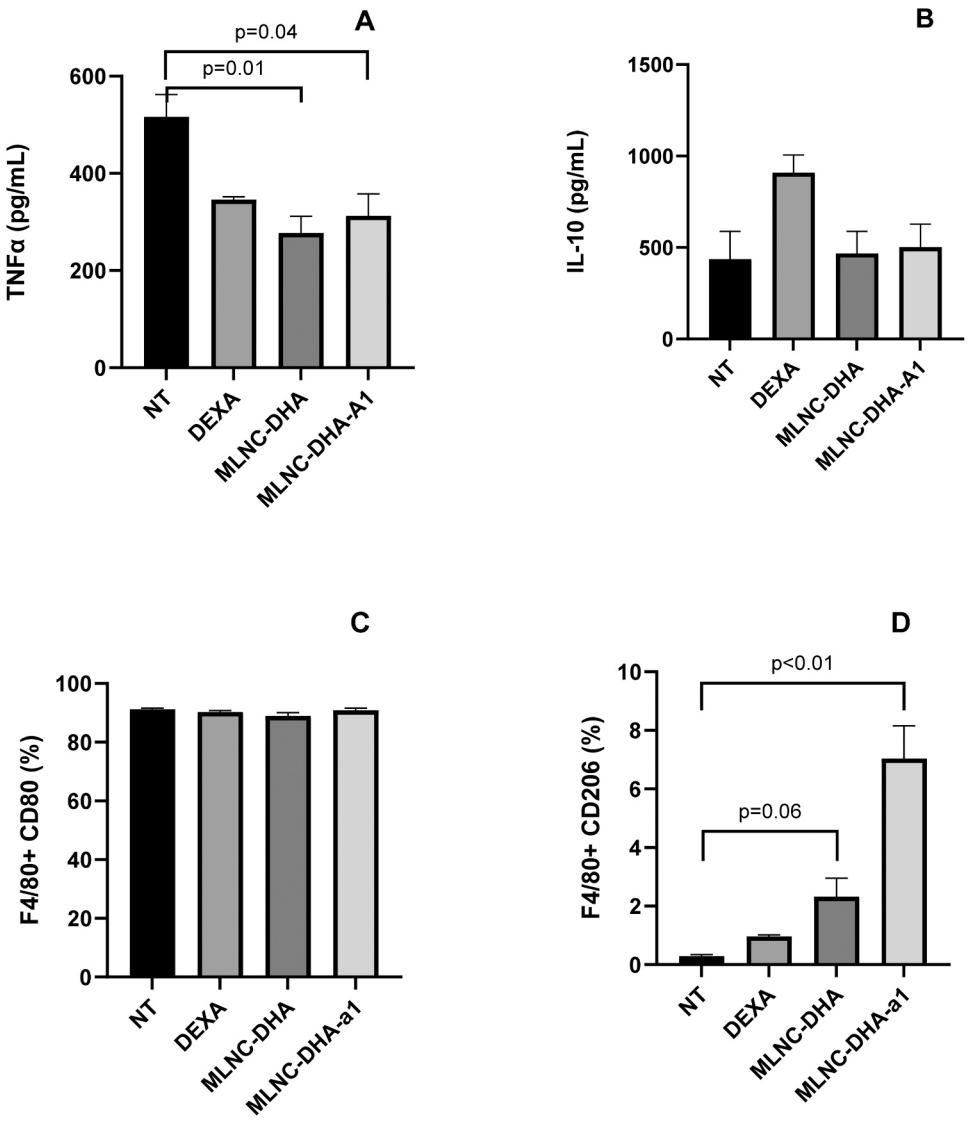

Fig. 4. Cytokines concentration and polarization in C57BL/6 mouse bone marrow-derived macrophages (BMDM). Assays were performed with dexamethasone (500 ng/mL) (DEXA), MLNC-DHA (0.75×10^{11} particles/mL), MLNC-DHA-a1 (0.75 ×1011 particles/mL containing 200 μg/mL of Anti-PECAM-1 and without any treatment (NT) for 48 h. Fig. 4A: TNFα (pg/mL); $p = 0.02$; Fig. 4 B: IL-10 (pg/mL); $p = 0.29$; Fig. 4C: Percentage of F4/80 + CD80 double positive cells (M1), ($p = 0.25$) and Fig. 4D: Percentage of F4/80 + and CD206 double positive cells (M2), ($p < 0.01$). Vertical bars are mean ± SEM (NT, n = 3; DEXA, n = 2; MLNC-DHA, n = 6 and MLNC-DHA-a1, n = 5 for cytokines and NT, n = 5; DEXA, n = 4; MLNC-DHA, n = 6 and MLNC-DHA-a1, n = 6 for polarization). Treatments were compared by One-way ANOVA and Tukey HSD or equivalent non parametric Kruskal Wallis analysis.

host defense cells [35,39]. The ability of RAW macrophages to engulf booth MLNC-DHA and MLNC-DHA-a1 nanocapsules, as shown in Fig. 3, may result from a balance between their spherical shape associated with non-ionic surface charge. This combination may influence their further *in vivo* application.

In our study using mice-derived BMDM cells, it was not observed any differences in the M1%, as measured using the F4/80 + CD80 marker (Fig. 4C) or in the IL-10 concentration (Fig. 4B), which is typically found in lower levels in M1 phenotype [40,41]. Taking into account the intense M2 polarization showed by MLNC-DHA-a1 (7.04%) compared with NT (0.30%), as measured using F4/80 + CD206 marker (Fig. 4D), followed by the reduced secretion of TNFα (Fig. 4A) observed to both MLNC-DHA and MLNC-DHA-a1, our results suggest that DHA present in the algae oil composing the lipid core of the nanocapsules has the potential to reduce the inflammatory microenvironment and improve macrophage functionality.

Based on these *in vitro* results, the nanocapsules were evaluated using an animal model. A limited number of *in vivo* studies has investigated the biological effects of omega-3 fatty acids-containing nanomaterials in cardiovascular diseases and cancer [20,42] and to the best of our knowledge, none of these studies has applied algae oil in the core of a nanocapsule surface-functionalized with anti-PECAM-1. For this reason, there was any previous information about a safe dose for intervention. Our data showed 5.36×10^8 surface-functionalized (anti-PECAM-1) metal-complex multi-wall nanocapsules containing 12 μL DHA/mL were well tolerated by $LDL^{(-/-)}$ mice, since all groups had similar diet intake and body weight gain, without no signs of local inflammation following caudal vein injections. Furthermore, data from fatty acids profile, relative weight and cytokines concentration suggested that our nanocapsules did not accumulate in the liver, causing any inflammatory reaction.

Conversely, MLNC-DHA-a1 nanocapsules promoted a modulation in the cytokine profile in the plasma, suggesting an inflammatory activation due to the increased release of IL-6 and IL-1β (Figs. 5A and 5B). However, there were no change observed in TNFα (Fig. 5C), while an increase was verified to anti-inflammatory IL-10 (Fig. 5C). It is important to note that several aspects of the nanocarriers can interact with the immune system, remembering that host defenses are the leading causes of nanocarriers side effects [35,43]. It has been reported that the size between 100 and 200 nm has the highest potential for prolonged circulation because this range is large enough to avoid the uptake by the liver, but small enough to avoid filtration in the spleen, thereby extending circulation and providing more opportunities for target engagement [43]. In a study reported by Deshpande et al. [44] flaxseed oil containing 17-β-estradiol was nanoencapsulated and functionalized with CREKA-peptides due to their specific binding affinity to

Table 1
Major fatty acid composition determined in plasma and liver homogenate of the experimental groups after 32 weeks of treatment.

	CONT	DHA-D	MLNC-DHA-a1	P[a] value
Plasma (%)				
C16:0	33.41 ± 1.86	32.49 ± 2.23	33.40 ± 1.19	*0.92*
C16:1 n7	2.56 ± 0.24	1.92 ± 0.09	2.29 ± 0.19	*0.15*
C17:0	0.02 ± 0.02	0.06 ± 0.06	ND	*0.35*
C18:0	17.09 ± 1.94	19.38 ± 2.24	19.53 ± 0.81	*0.44*
C18:1 n9	27.37 ± 2.65	24.02 ± 4.48	23.77 ± 1.34	*0.52*
C18:2 n6 (LNA)	14.73 ± 1.70	15.87 ± 1.20	14.88 ± 0.88	*0.83*
C18:3 n3 (ALA)	ND[a]	0.43 ± 0.05[b]	0.23 ± 0.05[ab]	*< 0.01*
C18:3 n6	0.15 ± 0.08	0.12 ± 0.08	0.20 ± 0.06	*0.66*
C20:3 n6	ND	0.12 ± 0.12	0.07 ± 0.07	*0.52*
C20:4 n6 (AA)	3.76 ± 0.71	3.78 ± 0.68	4.35 ± 0.41	*0.67*
C20:0	0.04 ± 0.02	0.03 ± 0.03	ND	*0.20*
C20:5 n3 (EPA)	0.03 ± 0.02	0.01 ± 0.01	ND	*0.19*
C22:6 n3 (DHA)	0.78 ± 0.37	1.78 ± 0.43	1.29 ± 0.24	*0.18*
Liver (%)				
C16:0	38.22 ± 2.81[a]	35.03 ± 0.62[ab]	32,22 ± 0.82[b]	*0.04*
C16:1 n7	1.43 ± 0.13[a]	2.01 ± 0.12[ab]	2.38 ± 0.22[b]	*0.01*
C18:0	19.81 ± 2.64	20.19 ± 1.39	18.76 ± 0.73	*0.78*
C18:1 n9	18.72 ± 3.04	20.48 ± 1.58	25.07 ± 0.92	*0.05*
C18:2 n6 (LNA)	16.14 ± 1.82	14.87 ± 1.03	15.19 ± 0.89	*0.78*
C18:3 n3 (ALA)	0.49 ± 0.29	0.26 ± 0.08	0.24 ± 0.05	*0.48*
C18:3 n6	0.23 ± 0.08	0.10 ± 0.07	0.20 ± 0.06	*0.48*
C20:4 n6 (AA)	4.03 ± 0.48	4.82 ± 0.62	4.45 ± 0.30	*0.67*
C22:6 n3 (DHA)	0.89 ± 0.40[a]	2.23 ± 0.29[b]	1.47 ± 0.22[ab]	*0.03*

[a] Values were expressed as mean ± SEM (CONT, n = 6; DHA-D, n = 5 and MLNC-DHA-a1, *n* = 9). Treatments were compared by One-way ANOVA and Tukey HSD or equivalent non parametric Kruskal Wallis analysis. P values refer to the comparison among the four groups. Values followed by the same letter do not differ ($p < 0.05$).

Table 2
Biochemical parameters observed in the experimental groups after 32 weeks of treatment.

	CONT	DHA-D	LNC-MCT	MLNC-DHA-a1	P value[a]
Plasma					
Glucose (mg/dL)	151.70 ± 19.50	190.50 ± 21.39	124.86 ± 15.56	148.20 ± 12.03	*0.08*
TC (mg/dL)	191.40 ± 18.35	230.25 ± 36.52	173.07 ± 13.54	195.40 ± 9.26	*0.74*
LDL (mg/dL)	92.40 ± 10.72	84.00 ± 8.71	78.43 ± 6.83	89.67 ± 5.52	*0.56*
HDL (mg/dL)	39.30 ± 2.51	43.50 ± 2.20	42.36 ± 3.02	44.60 ± 2.39	*0.57*
TG (mg/dL)	85.30 ± 12.42	101.25 ± 20.79	68.29 ± 5.17	85.33 ± 7.49	*0.39*
ALT (mg/dL)	69.20 ± 12.61	59.25 ± 9.21	44.00 ± 7.04	55.53 ± 6.31	*0.22*
AST (mg/dL)	168.80 ± 35.89	136.50 ± 17.79	117.64 ± 14.22	129.33 ± 14.46	*0.78*
Liver					
Relative weight (%)	0.04 ± 0.01	0.04 ± 0.01	0.04 ± 0.01	0.04 ± 0.01	*0.33*
Cytokines (liver)					
IL1β (pg/mL)	0.47 ± 0.07	0.57 ± 0.07	0.65 ± 0.05	0.61 ± 0.07	*0.29*
IL-6 (pg/mL)	4.70 ± 0.36	3.91 ± 0.34	4.97 ± 0.44	4.25 ± 0.33	*0.24*
IL-10 (pg/mL)	2.86 ± 0.38	2.26 ± 0.20	3.78 ± 0.43	3.16 ± 0.44	*0.05*
TNFα (pg/mL)	0.24 ± 0.03	0.25 ± 0.02	0.25 ± 0.02	0.23 ± 0.02	*0.90*

[a] *Values were expressed as mean ± SEM (CONT, n = 11; DHA-D, n = 9; LNC-MCT, n = 14 and MLNC-DHA-a1, n = 15).* Treatments were compared by One-way ANOVA and Tukey HSD or equivalent non parametric Kruskal Wallis analysis. P values refer to the comparison among the four groups.

atherosclerotic plaque. Similar to our protocol, the nanocapsules were intravenously injected in ApoE $^{(-/-)}$ mice fed a high-fat diet for 10 weeks, totalizing 10 doses at the end of the experiment. The authors observed that the weight gain of animals was not affected by the treatment, and plasma ALT and AST concentrations remained within the normal range. Sha et al. [42] developed a nanoparticle derived from macrophage membrane-coated liposome, aiming to improve efferocytosis in the arterial wall. They observed good compatibility, prolonged blood circulation time, and no cytotoxicity in MTT assays. Thus, the observed weight gain and dietary tolerance in our study may be attributed to a combination of MLNC-DHA-a1 size (164 nm), spherical shape and an adequate dose.

Under normal circumstances, opsonization by immunoglobulins and complement proteins begins immediately upon contact of the nanoparticles with plasma, followed by mechanical filtration in the spleen [43]. Although there is no data about pharmacokinetic and pharmacodynamics properties in our research, it is plausible that our nanocapsules infiltrated the inflamed endothelium, spleen or other tissue and cells that express PECAM-1 and have triggered the immune response observed in plasma.

The systemic inflammation observed in our study may be caused by the purity of algae oil in the lipid core, the antibody in the nanocapsule surface or the chitosan applied in the wall, since group LNC-MCT did not show the same behavior. In fact, LNC-MCT group was included in our protocol because there were previous studies reporting its safety when applied in animal models [38,45]. Platelet-Endothelial Cell Adhesion Molecule-1 (PECAM-1) is a protein widely expressed, to different degrees, on most leukocyte subtypes, platelets and endothelial cells, where its expression is primarily concentrated at junctions between adjacent cells [46]. It has been reported that under an inflammatory condition, such as those observed in atherosclerosis, PECAM-1 increases the junction permeability between the endothelial cells, facilitating the infiltration of immune cells into the inflamed intima [47]. However, the toxicity of anti-PECAM-1 has shown controversial results. Fig. 2 shows that 200 μg/mL of Anti-PECAM-1 did not reduce viability when evaluated in RAW 264.7 cells. In another study, PECAM-targeted polymer nanocarriers injected into mice did not show toxicity [48]. Despite this, it was observed a systemic release of pro-inflammatory cytokines after intravenous administration of anti-PECAM-1 [49]. This adverse result could be attributed to the fact that the engagement of the extracellular domains of PECAM-1 can compromise barrier function or lead to bidirectional signaling, with consequences toward cell survival, affecting junctional integrity and leukocytes and platelet adhesion. Thus, more studies involving anti-PECAM must be carried out to establish PECAM-1 targeted drugs safety, considering that nanoparticle binding can lead to unexpected biological consequences.

Conversely, chitosan has been considered non-toxic, biocompatible and biodegradable. However, caution should be taken regarding its interactions with biological systems, which depends on concentration, deacetylation degree and positive charge [50]. In a study involving algae oil, two samples obtained from Schizochytrium sp, were submitted to a battery of in vivo and in vitro genotoxicity tests. The results indicated that the oil was well tolerated and had no adverse effects at the highest dose of 3305 and 3679 mg/kg bw/day, for male and female rats, respectively [51], that is about 120 times higher than the dose applied in our study. According to the supplier, the algae oil applied in our nanocapsules contained DHA in the form of triacylglycerol along with ascorbyl palmitate (250 ppm) and tocopherol (250 ppm), being certified as safe for the intended use. However, considering the direct intravenous injection, a higher degree of purity than those approved for dietary use should be evaluated in further studies. Besides the purity, the amount of DHA injected in the plasma by the nanocapsules could trigger an immune system response. In our study, fatty acids were expressed as a percentage, and the proportion found in plasma similar to the proportion found in liver. It was estimated that each application of the nanocapsules provided about 2.8 μg DHA kg bw. Thus, quantitative

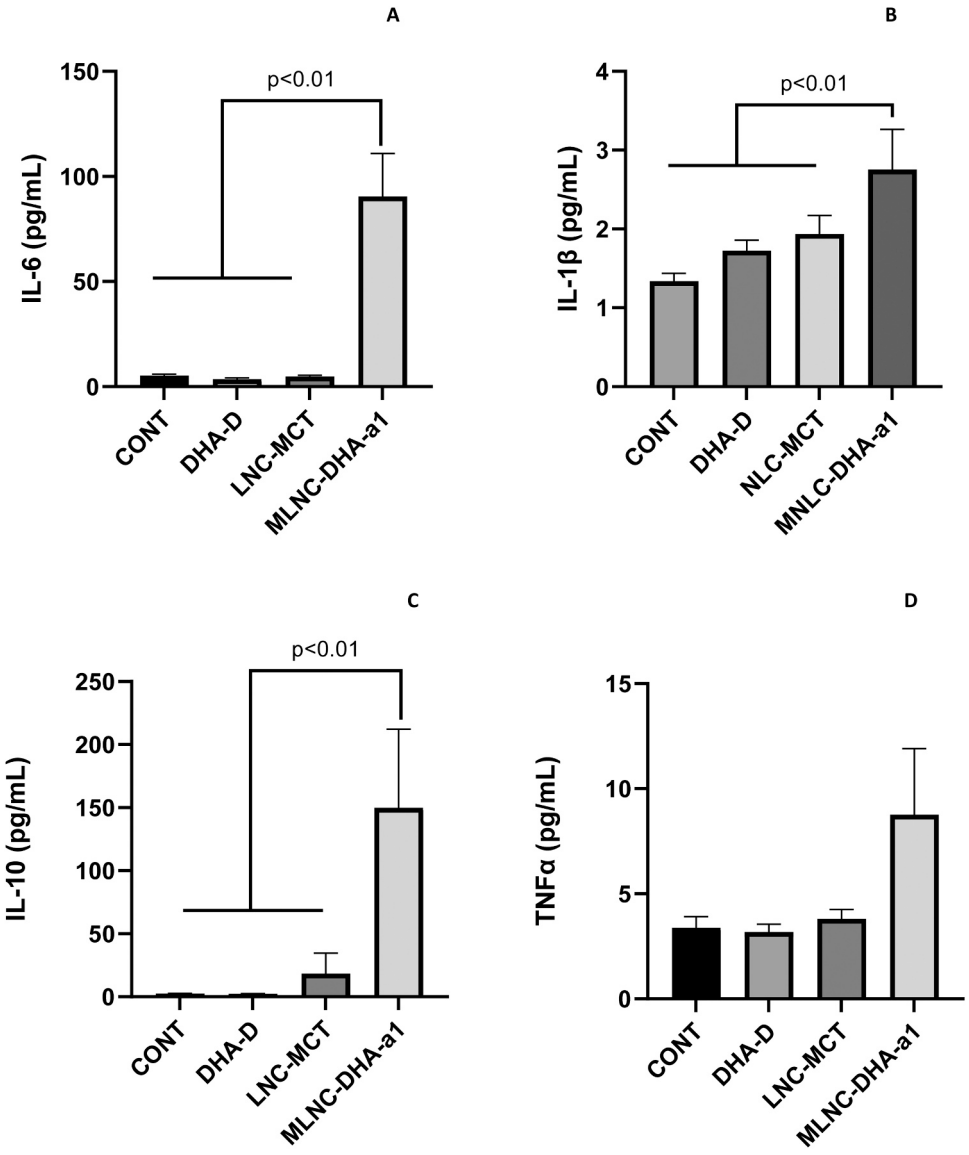

Fig. 5. Cytokines concentration analyzed in plasma. Fig. 5A: IL-6 concentration (pg/mL); Fig. 5B: IL-1β concentration (pg/mL); Fig. 5C: IL-10 concentration (pg/mL); and Fig. 5D: TNFα concentration (pg/mL). Vertical bars are mean ± SEM (CONT, n = 10; DHA, n = 8; LNC-MCT, n = 14 and MLNC-DHA-a1, n = 12). Treatments were compared by One-way ANOVA and Tukey HSD or equivalent non parametric Kruskal Wallis analysis.

determination of DHA in plasma should be done in the next studies.

Concerning the oral supplementation of algae oil, it was also expected that the replacement of AA by EPA and DHA in membrane phospholipids could promote a reduction in the substrate necessary to synthesize series 2 and 4 eicosanoids, able to facilitate acquired immunity and induce long-lasting immune inflammation [52]. However, there was no difference in cytokines concentration comparing DHA-D and CONT groups, suggesting that the supplementation was insufficient to reduce systemic inflammation once the stimulus was discontinued. Toko et al. [53] observed a suppression in the expression of pro-inflammatory cytokines in the heart of mice supplemented with EPA and DHA. However, it is also worth noting that they applied a dose much higher (1500.00 mg/kg. bw/day) than the dose used in our model (10.00 mg/kg.bw/say). In other study, C57BL/6 mice were supplemented with 200 mg/kg.bw of algae oil and intestinal damage was induced by Ceftriaxone sodium. After 8 days, the animals showed inhibition of the pro-inflammatory cytokine tumor necrosis factor (TNF)-α, interleukin (IL)− 6 and myeloperoxidase (MPO) activity [54]. Xu et al. [55] induced colitis in Male C57BL/6 mice using 2.5% DSS and followed them with 2 weeks of treatment with algal oil (250 or 500 mg/kg/day). The authors concluded that algal oil could be applied in the development of therapeutics for intestinal inflammation.

In fact, there is currently no evidence to suggest that the control of chronic inflammation is dose-related [56]. The solution applied in our study contained 1.34×10^{13} nanocapsules/mL with 12 μL/mL of algae oil (35.13 ± 0.35% DHA). This solution was injected at a rate of 40 μL/animal once a week for 8 weeks. This amount corresponded to 8.9×10^{-19} mols/animal/week, based on the Avogadro's number. The results showed that MLNC-DHA-a1 nanocapsules were well-tolerated *in vivo*, but activated an immune response, increasing the cytokines concentration in the plasma. Considering that this immune response is a limitation to clinical trials, future experiments should aim to identify which compound within the nanocapsules was responsible for activating the immune response.

4. Conclusion

Our findings suggest that algae oil with a higher DHA content, incorporated as part of the lipid core within the nanocapsules, appears to improve the macrophage phenotype, being a potential therapy for

controlling chronic inflammation However, MLNC-DHA-a1 nanocapsules increased pro-inflammatory cytokines in the plasma. Thus, further studies should identify which compounds triggered the immune response and to assess whether this effect might have adverse implications for susceptibility to infections.

Ethics approval and informed consent

All the protocols were approved by the Institutional Animal Care and Use Committee of the Faculty of Pharmaceutical Sciences, University of São Paulo (CEUA/FCF 555).

Funding

This study was supported by The State of São Paulo Research Foundation (FAPESP) (Scholarship and Research Grant 2019/21029–3, 2021/02021–1, 2021/08196–8) and National Council for Scientific and Technological Development (CNPq – Scholarship: 166541/2017–6).

CRediT authorship contribution statement

Conceptualization, I.A.C.; methodology, I.P.; S.J.C.; M.C.L.; A.R.P and S.S.G; formal analysis, I.P.; S.C.J.; K.B.; B.C.;M.K.U.; K.A.; resources, I.A.C.; writing, I.A.C; M.C.L.;I.P.; review and editing, I.P.; M.C.L. All authors have read and agreed to the published version of the manuscript.

Declaration of Competing Interest

The author reports no conflicts of interest in this work.

Data Availability

Data will be made available on request.

Appendix A. Supporting information

Supplementary data associated with this article can be found in the online version at doi:10.1016/j.biopha.2023.115474.

References

[1] L. Chen, H. Deng, H. Cui, et al., Inflammatory responses and inflammation-associated diseases in organs, Oncotarget 9 (6) (2017) 7204–7218, https://doi.org/10.18632/oncotarget.23208.
[2] D. Furman, J. Campisi, E. Verdin, et al., Chronic inflammation in the etiology of disease across the life Span, Nat. Med 25 (12) (2019) 1822–1832, https://doi.org/10.1038/s41591-019-0675-0.
[3] A. Christ, M. Lauterbach, E. Latz, Western Diet and the Immune System: An Inflammatory Connection, Immunity 51 (5) (2019) 794–811, https://doi.org/10.1016/j.immuni.2019.09.020.
[4] P. Stenvinkel, M. Ketteler, R.J. Johnson, B. Lindholm, R. Pecoits-Filho, M. Riella, O. Heimbürger, T. Cederholm, M. Girndt, IL-10, IL-6, and TNF-α: Central factors in the altered cytokine network of uremia—The good, the bad, and the ugly, Kidney Int. 67 (4) (2005) 1216–1233, https://doi.org/10.1111/j.1523-1755.2005.00200.x.
[5] Hangai, S., Ao, T., Kimura, Y., Matsuki, K., Kawamura, T., Negishi, H., Nishio, J., Kodama, T., Taniguchi, T. and Yanai, H. (2016). PGE2 induced in and released by dying cells functions as an inhibitory DAMP. Proceedings of the National Academy of Sciences of the United States of America, [online] 113(14): 3844–3849. doi:10.1073/pnas.1602023113.
[6] M.D. Howard, E.D. Hood, B. Zern, V.V. Shuvaev, T. Grosser, V.R. Muzykantov, Nanocarriers for vascular delivery of anti-inflammatory agents, Annu. Rev. Pharmacol. Toxicol. 54 (2014) 205–226, https://doi.org/10.1146/annurev-pharmtox-011613-140002.
[7] T. Rhen, J.A. Cidlowski, Antiinflammatory action of glucocorticoids — new mechanisms for old drugs, N. Engl. J. Med 353 (2005) 1711–1723, https://doi.org/10.1056/NEJMra050541.
[8] H.E. Vonkeman, M.A.F.J. van de Laar, Nonsteroidal anti-inflammatory drugs: adverse effects and their prevention, Semin. Arthritis Rheum. 39 (2010) 294–312, https://doi.org/10.1016/j.semarthrit.2008.08.001.
[9] S. Wongrakpanich, A. Wongrakpanich, K. Melhado, J. Rangaswami, A comprehensive review of non-steroidal anti-inflammatory drug use in the elderly ([online]), Aging Dis. 9 (1) (2018) 143, https://doi.org/10.14336/ad.2017.0306.
[10] ANON.
[11] J.S. Chandan, D.T. Zemedikun, R. Thayakaran, N. Byne, S. Dhalla, D. Acosta-Mena, K.M. Gokhale, T. Thomas, C. Sainsbury, A. Subramanian, J. Cooper, A. Anand, K. O. Okoth, J. Wang, N.J. Adderley, T. Taverner, A.K. Denniston, J. Lord, G. N. Thomas, C.D. Buckley, Nonsteroidal antiinflammatory drugs and susceptibility to COVID-19, Arthritis Rheumatol. 73 (2021) 731–739, https://doi.org/10.1002/art.41593.
[12] W. Zhang, Y. Zhao, F. Zhang, Q. Wang, T. Li, Z. Liu, J. Wang, Y. Qin, X. Zhang, X. Yan, X. Zeng, S. Zhang, The use of anti-inflammatory drugs in the treatment of people with severe coronavirus disease 2019 (COVID-19): the perspectives of clinical immunologists from China, Clin. Immunol. 214 (2020), 108393, https://doi.org/10.1016/j.clim.2020.108393.
[13] P.C. Calder, Omega-3 fatty acids and inflammatory processes: from molecules to man, Biochem Soc. Trans. 45 (5) (2017) 1105–1115, https://doi.org/10.1042/BST20160474.
[14] P.C. Calder, Omega-3 fatty acids and inflammatory processes, Nutrients 2 (3) (2010) 355–374, https://doi.org/10.3390/nu2030355.
[15] R. Bosviel, L. Joumard-Cubizolles, G. Chinetti-Gbaguidi, D. Bayle, C. Copin, N. Hennuyer, I. Duplan, B. Staels, G. Zanoni, A. Porta, L. Balas, J.-M. Galano, C. Oger, A. Mazur, T. Durand, C. Gladine, DHA-derived oxylipins, neuroprostanes and protectins, differentially and dose-dependently modulate the inflammatory response in human macrophages: putative mechanisms through PPAR activation, Free Radic. Biol. Med. 103 (2017) 146–154, https://doi.org/10.1016/j.freeradbiomed.2016.12.018.
[16] H.Y. Chang, H.N. Lee, W. Kim, Y.J. Surh, Docosahexaenoic acid induces M2 macrophage polarization through peroxisome proliferator-activated receptor γ activation, Life Sci. 120 (2015) 39–47, https://doi.org/10.1016/j.lfs.2014.10.014.
[17] K.T. Feehan, D.W. Gilroy, Is resolution the end of inflammation? Trends Mol. Med 25 (3) (2019) 198–214, https://doi.org/10.1016/j.molmed.2019.01.006.
[18] B.E. Sansbury, M. Spite, Resolution of Acute Inflammation and the Role of Resolvins in Immunity, Thrombosis, and Vascular Biology, 24, Circ. Res 119 (1) (2016) 113–130, https://doi.org/10.1161/CIRCRESAHA.116.307308.
[19] Y. Yan, W. Jiang, T. Spinetti, A. Tardivel, R. Castillo, C. Bourquin, R. Zhou, Omega-3 fatty acids prevent inflammation and metabolic disorder through inhibition of NLRP3 inflammasome activation, Immunity 38 (6) (2013) 1154–1163, https://doi.org/10.1016/j.immuni.2013.05.015.
[20] S. Serini, R. Cassano, S. Trombino, G. Calviello, Nanomedicine-based formulations containing ω-3 polyunsaturated fattyacids: potential application in cardiovascular and neoplastic diseases, Int J. Nanomed. 14 (2019) 2809–2828, https://doi.org/10.2147/IJN.S197499.
[21] P.M. Ridker, B.M. Everett, T. Thuren, et al., Anti-inflammatory therapy with canakinumab for atherosclerotic disease, N. Engl. J. Med 377 (12) (2017) 1119–1131, https://doi.org/10.1056/NEJMoa1707914.
[22] H. Wang, Y. Zhou, Q. Sun, et al., Update on nanoparticle-based drug delivery system for anti-inflammatory treatment, Front Bioeng. Biotechnol. 17 (9) (2021), 630352, https://doi.org/10.3389/fbioe.2021.630352.
[23] M. de Castro Leão, A. Raffin Pohlmann, A. de Cristo Soares Alves, et al., Docosahexaenoic acid nanoencapsulated with anti-PECAM-1 as co-therapy for atherosclerosis regression, Eur. J. Pharm. Biopharm. 159 (2021) 99–107, https://doi.org/10.1016/j.ejpb.2020.12.016.
[24] S. Schlager, N. Vujic, M. Korbelius, et al., Lysosomal lipid hydrolysis provides substrates for lipid mediator synthesis in murine macrophages, Oncotarget 8 (25) (2017) 40037–40051, https://doi.org/10.18632/oncotarget.16673.
[25] L. Ménégaut, A. Jalil, C. Thomas, D. Masson, Macrophage fatty acid metabolism and atherosclerosis: The rise of PUFAs, Atherosclerosis 291 (2019) 52–61, https://doi.org/10.1016/j.atherosclerosis.2019.10.002.
[26] C.N. Serhan, B.D. Levy, Resolvins in inflammation: emergence of the pro-resolving superfamily of mediators, J. Clin. Invest 128 (7) (2018) 2657–2669, https://doi.org/10.1172/JCI97943.
[27] S.A. Amici, J. Dong, M. Guerau-de-Arellano, Molecular mechanisms modulating the phenotype of macrophages and microglia, Front Immunol. 8 (2017) 1520, https://doi.org/10.3389/fimmu.2017.01520. PMID: 29176977; PMCID: PMC5686097.
[28] S. Sandri, C.B. Hebeda, R.A. Loiola, et al., Direct effects of poly(ε-caprolactone) lipid-core nanocapsules on human immune cells, Nanomed. (Lond.) 14 (11) (2019) 1429–1442, https://doi.org/10.2217/nnm-2018–0484 W.
[29] W. Ying, P.S. Cheruku, F.W. Bazer, S.H. Safe, B. Zhou, Investigation of macrophage polarization using bone marrow derived macrophages, J. Vis. Exp. 76 (2013) 50323, https://doi.org/10.3791/50323.
[30] P.G. Reeves, F.H. Nielsen, G.C. Fahey, AIN-93 purified diets for laboratory rodents: final report of the American institute of nutrition ad hoc writing committee on the reformulation of the AIN-76A rodent diet, J. Nutr. 123 (11) (1993) 1939–1951, https://doi.org/10.1093/jn/123.11.1939.
[31] T. Küster, B. Zumkehr, C. Hermann, et al., Voluntary ingestion of antiparasitic drugs emulsified in honey represents an alternative to gavage in mice, J. Am. Assoc. Lab Anim. Sci. 51 (2) (2012) 219–223.
[32] P.M. Kris-Etherton, W.S. Harris, L.J. Appel, AHA nutrition committee. american heart association. Omega-3 fatty acids and cardiovascular disease: new recommendations from the american heart association, Arterioscler. Thromb. Vasc. Biol. 23 (2) (2003) 151–152, https://doi.org/10.1161/01.atv.0000057393.97337.ae.
[33] Y.-L. Hong, S.-L. Yeh, C.-Y. Chang, et al., Total plasma malondialdehyde levels in 16 taiwanese college students determined by various thiobarbituric acid tests and

an improved high-performance liquid chromatography-based method, Clin. Biochem 33 (8) (2000) 619–625, https://doi.org/10.1016/s0009-9120(00)00177-6.
[34] N. Shirai, H. Suzuki, S. Wada, Direct methylation from mouse plasma and from liver and brain homogenates, Anal. Biochem 343 (1) (2005) 48–53, https://doi.org/10.1016/j.ab.2005.04.037.
[35] H. Parhiz, M. Khoshnejad, J.W. Myerson, et al., Unintended effects of drug carriers: Big issues of small particles, Adv. Drug Deliv. Rev. 130 (2018) 90–112, https://doi.org/10.1016/j.addr.2018.06.023.
[36] M.F. Cavalcante, M.D. Adorne, W.M. Turato, et al., scFv-Anti-LDL(-)-metal-complex multi-wall functionalized-nanocapsules as a promising tool for the prevention of atherosclerosis progression, Front Med (Lausanne) 8 (2021), 652137, https://doi.org/10.3389/fmed.2021.652137.
[37] C.B. Michalowski, M.D. Arbo, L. Altknecht, et al., Oral treatment of spontaneously hypertensive rats with captopril-surface functionalized furosemide-loaded multi-wall lipid-core nanocapsules, Pharmaceutics 12 (1) (2020) 80, https://doi.org/10.3390/pharmaceutics12010080.
[38] F.A. Bruinsmann, A. de Cristo Soares Alves, A. de Fraga Dias, et al., Nose-to-brain delivery of simvastatin mediated by chitosan-coated lipid-core nanocapsules allows for the treatment of glioblastoma in vivo, Int J. Pharm. 616 (2022), 121563, https://doi.org/10.1016/j.ijpharm.2022.121563.
[39] P.M. Glassman, J.W. Myerson, L.T. Ferguson, et al., Targeting drug delivery in the vascular system: Focus on endothelium, Adv. Drug Deliv. Rev. 157 (2020) 96–117, https://doi.org/10.1016/j.addr.2020.06.013.
[40] G. Chinetti-Gbaguidi, S. Colin, B. Staels, Macrophage subsets in atherosclerosis, Nat. Rev. Cardiol. 12 (1) (2015) 10–17, https://doi.org/10.1038/nrcardio.2014.173.
[41] M. de Gaetano, D. Crean, M. Barry, O. Belton, M1- and M2-type macrophage responses are predictive of adverse outcomes in human atherosclerosis, Front Immunol. 7 (2016) 275, https://doi.org/10.3389/fimmu.2016.00275.
[42] X. Sha, Y. Dai, L. Chong, M. Wei, M. Xing, C. Zhang, et al., Pro-efferocytic macrophage membrane biomimetic nanoparticles for the synergistic treatment of atherosclerosis via competition effect, J. Nanobiotechnol. 20 (1) (2022) 506, https://doi.org/10.1186/s12951-022-01720-2.
[43] R.A. Petros, J.M. DeSimone, Strategies in the design of nanoparticles for therapeutic applications, Nat. Rev. Drug Discov. 9 (8) (2010) 615–627, https://doi.org/10.1038/nrd2591.
[44] D. Deshpande, S. Kethireddy, D.R. Janero, M.M. Amiji, Therapeutic efficacy of an ω-3-fatty acid-containing 17-β estradiol nano-delivery system against experimental atherosclerosis, PLoS One 11 (2) (2016), e0147337, https://doi.org/10.1371/journal.pone.0147337.
[45] M.T.P. de Oliveira, D.S. Coutinho, S.S. Guterres, A.R. Pohlmann, PMRE Silva, M. A. Martins, A. Bernardi, Resveratrol-loaded lipid-core nanocapsules modulate acute lung inflammation and oxidative imbalance induced by LPS in mice, Pharmaceutics 13 (5) (2021) 683, https://doi.org/10.3390/pharmaceutics13050683. PMID: 34068619; PMCID: PMC8151102.
[46] A. Woodfin, M.-B. Voisin, S. Nourshargh, PECAM-1: a multi-functional molecule in inflammation and vascular biology, Arterioscler. Thromb. Vasc. Biol. 27 (12) (2007) 2514–2523, https://doi.org/10.1161/ATVBAHA.107.151456.
[47] J.R. Privratsky, P.J. Newman, PECAM-1: regulator of endothelial junctional integrity, Cell Tissue Res 355 (3) (2014) 607–619, https://doi.org/10.1007/s00441-013-1779-3.
[48] T.D. Dziubla, V.V. Shuvaev, N.K. Hong, et al., Endothelial targeting of semi-permeable polymer nanocarriers for enzyme therapies, Biomaterials 29 (2) (2008) 215–227, https://doi.org/10.1016/j.biomaterials.2007.09.023.
[49] R.Y. Kiseleva, C.F. Greineder, C.H. Villa, et al., Vascular endothelial effects of collaborative binding to platelet/endothelial cell adhesion molecule-1 (PECAM-1), Sci. Rep. 8 (1) (2018) 1510, https://doi.org/10.1038/s41598-018-20027-7.
[50] L.A. Frank, G.R. Onzi, A.S. Morawski, et al., Chitosan as a coating material for nanoparticles intended for biomedical applications, React. Funct. Polym. 147 (11) (2020), 104459, https://doi.org/10.2174/1389200218666170925122201.
[51] D. Schmitt, N. Tran, J. Peach, et al., Toxicologic evaluation of DHA-Rich algal oil: genotoxicity, acute and subchronic toxicity in rats, Food Chem. Toxicol. 50 (10) (2012) 3567–3576, https://doi.org/10.1016/j.fct.2012.07.054.
[52] T. Aoki, S. Narumiya, Prostaglandins and chronic inflammation, Trends Pharm. Sci. 33 (6) (2012) 304–311, https://doi.org/10.1016/j.tips.2012.02.004.
[53] H. Toko, H. Morita, M. Katakura, et al., Omega-3 fatty acid prevents the development of heart failure by changing fatty acid composition in the heart, Sci. Rep. 10 (1) (2020) 15553, https://doi.org/10.1038/s41598-020-72686-0.
[54] H. Zhang, Z. Xu, W. Chen, F. Huang, S. Chen, X. Wang, C. Yang, Algal oil alleviates antibiotic-induced intestinal inflammation by regulating gut microbiota and repairing intestinal barrier, Front Nutr. 9 (2023) 1081717, https://doi.org/10.3389/fnut.2022.1081717. PMID: 36726819; PMCID: PMC9884693.
[55] Z. Xu, H. Tang, F. Huang, et al., Algal Oil Rich in n-3 PUFA Alleviates DSS-induced colitis via regulation of gut microbiota and restoration of intestinal barrier, Front. Microbiol (2020) 16, https://doi.org/10.3389/fmicb.2020.615404.
[56] A.C. Skulas-Ray, P.M. Kris-Etherton, W.S. Harris, et al., Dose-response effects of omega-3 fatty acids on triglycerides, inflammation, and endothelial function in healthy persons with moderate hypertriglyceridemia, Am. J. Clin. Nutr. 93 (2) (2011) 243–252, https://doi.org/10.3945/ajcn.110.